Steam Turbine Critical Crack Evaluation and Ranking Cracks to Prioritize Inspection

G. Thorwald, V. Garcia, R. Bentley, and O. Kwon

Quest Integrity

***Abstract**: The objective of this paper is to evaluate postulated cracks in a power plant steam turbine and to rank the cracks to prioritize inspection. 3D crack meshes are used to model a range of crack sizes and to compute the crack front J-integral and stress intensity K trends versus crack size. The Abaqus/CAE geometry model is partitioned to insert the crack meshes, which are connected to the larger mesh using tied contact. Abaqus/Standard is used to compute the J-integral and K values for cracks at several locations and for several crack shapes in the steam turbine impulse wheel. Single cracks and interacting cracks are compared.*

Ranking the cracks by comparing their K values reveals the most severe crack location and crack shape. The critical crack size for the most severe crack case is determined using the Failure Assessment Diagram method. The evaluation points on the FAD plot are obtained using a combination of elastic K and elastic-plastic J-integral results. Determining the most severe crack location and critical crack size help inspectors prioritize where to look for cracking during the next scheduled maintenance and to select inspection methods to find cracks.

Engineers using Abaqus and 3D crack models benefit from computing accurate J-integral and K values to improve evaluations of actual or postulated cracks in structural components, such as a power plant steam turbine. Accurate analyses aid inspectors to plan their search for cracking and allows for greater confidence in the structure's integrity when the turbine is returned to service.

***Keywords**: Steam Turbine, Impulse Wheel Steeple, Failure Assessment Diagram, Fracture Failure, Plastic Collapse, Stress Intensity, KI, J-integral, Tied Contact, Sub-model, Abaqus/Standard, Abaqus/CAE, 3D Crack Mesh, Elastic-plastic analysis*

1. Introduction

Two common questions about structures with cracks are: will the crack cause an immediate failure, and if not, how soon will the crack grow to a size large enough to cause failure? The first question can be addressed using the Failure Assessment Diagram (FAD) method or a ductile tearing instability analysis, and the second question can be addressed by a fatigue crack propagation analysis (Thorwald and Wright 2016, Thorwald and Parietti 2016). In this paper the FAD method is used to examine postulated cracks in a power plant steam turbine shaft to help prioritize inspection during a maintenance shut-down and address the first question. After

describing the geometry, two crack examples are examined in more detail. The FAD method will be explained and used to determine a critical crack size.

A picture of the turbine shaft is shown in Figure 1; the turbine blades have been removed in this picture. The postulated cracks are modeled at seven locations in the impulse wheel steeple, which is near the middle of the shaft.

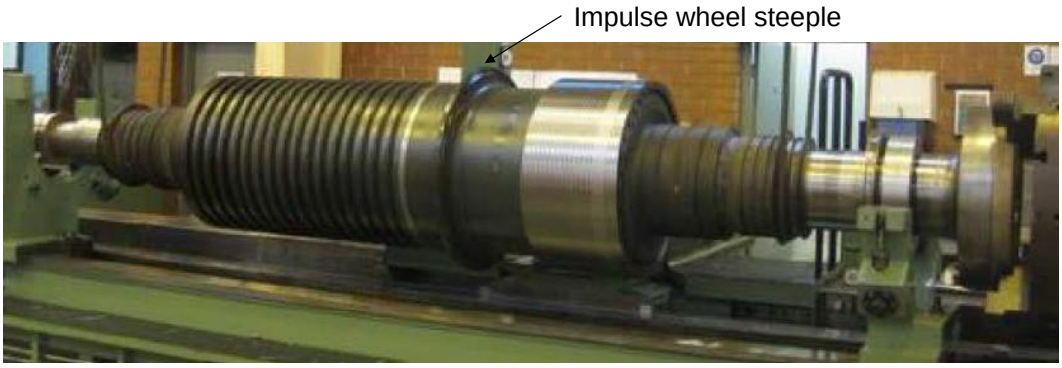

Figure 1. Steam turbine rotor shaft and steeple location.

The solid geometry model is a 45-degree segment, 1/8th symmetry, of the shaft and is shown in Figure 2. The solid model of the shaft was created using Abaqus/CAE, and the analyses were run using Abaqus/Standard (Abaqus 2017). Figure 3 shows the profile of the shaft and a close-up of the impulse wheel steeple. Centrifugal loading due to the shaft rotation is one of the loads applied to the shaft, indicated by vertical arrows along the length of the shaft. Figure 4 shows the pressure loads and traction loads applied to the shaft and steeple. The upstream pressure is higher than the downstream pressure. The pressure changes value at the middle top of the steeple. The traction loads applied to the bottom side of the steeple ledges are due to the centrifugal force from the impulse turbine blades and blade root block, which are omitted from the model. Figure 5 shows the profile of the blade root block that fits around the steeple, which is represented by the traction loads on the steeple ledges.

Figure 5 also shows the locations of the postulated cracks in the steeple. Seven crack cases were modeled to determine which cases are the most severe. The crack cases include: 360-degree circumferential partial depth cracks near the top of the steeple, axial cracks with a crack front across the steeple, combined axial-circumferential through cracks, corner cracks at the top of the steeple, combined axial-circumferential cracks for crack interaction, circumferential surface cracks near the top of the steeple, and combined axial-360-degree circumferential cracks for crack interaction. The 3D crack meshes were generated using the FEACrack software (FEACrack 2017) and inserted into the larger shaft mesh and connected using tied contact. Each crack case used a range of crack sizes to obtain a trend of stress intensity K values. The 3D crack models captured the complex nature of the crack shapes and reduce conservatism using approximate 2D models.

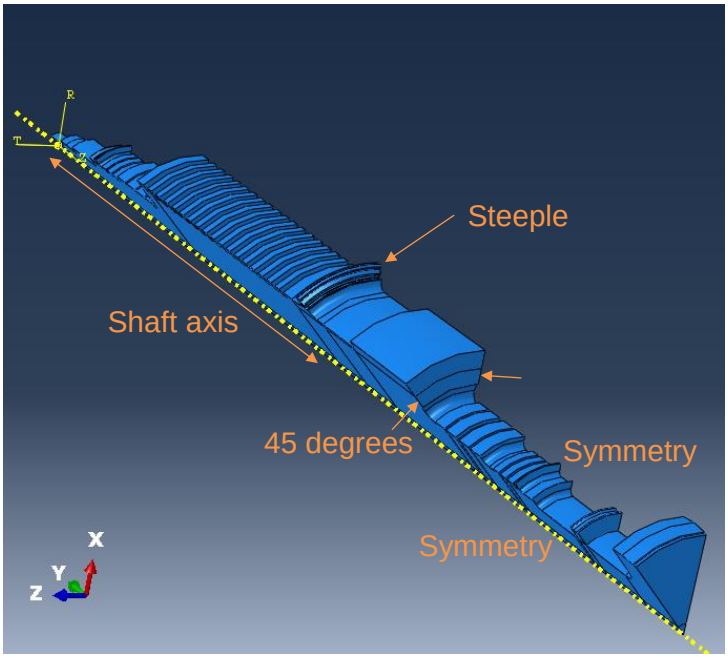

Figure 2. Abaqus/CAE solid model, 45-degree segment of shaft, 1/8th symmetry.

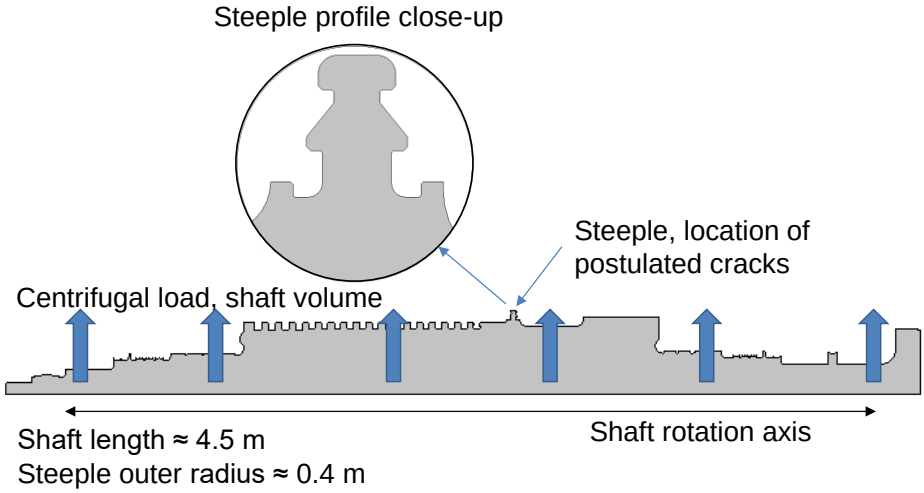

Figure 3. Rotor shaft profile, steeple location, centrifugal load.

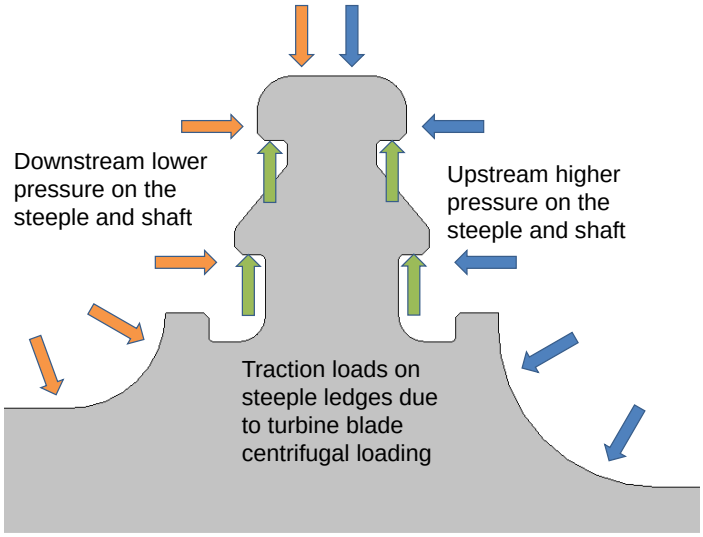

Figure 4. Pressure and traction loads on the steeple.

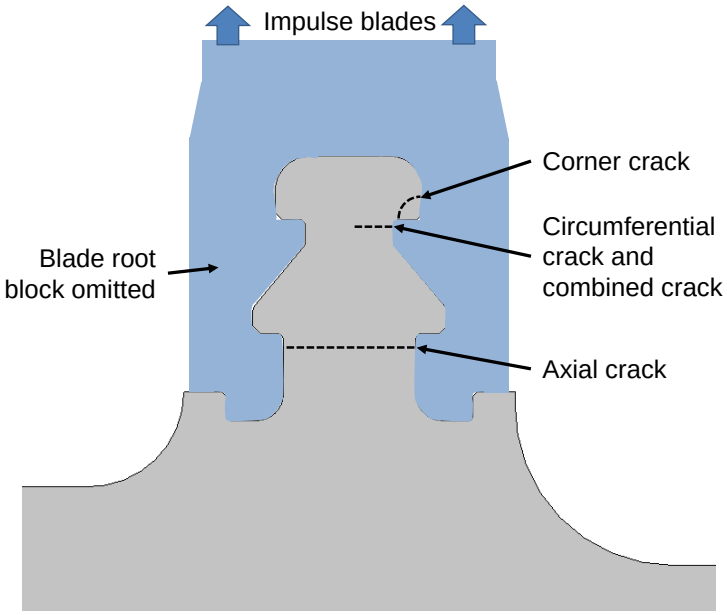

Figure 5. Blade root block around steeple and postulated crack locations.

Figure 6 shows a bar graph comparing the maximum crack front stress intensity K values for the largest crack size for each of the seven crack cases in the steeple. The 360-degree circumferential crack near the top of the steeple is the most severe case found, and is described in more detail in Section 2. It is also the one postulated crack case with a maximum stress intensity that exceeds the material toughness K_{mat} of 110 MPa √m. The FAD method is used in Section 4 to evaluate the 360-degree circumferential crack sizes to determine a critical crack size. The combined axial-circumferential crack is described further in Section 3. The other crack cases, including the crack interaction models, gave lower crack front stress intensity values and are not described further in this paper.

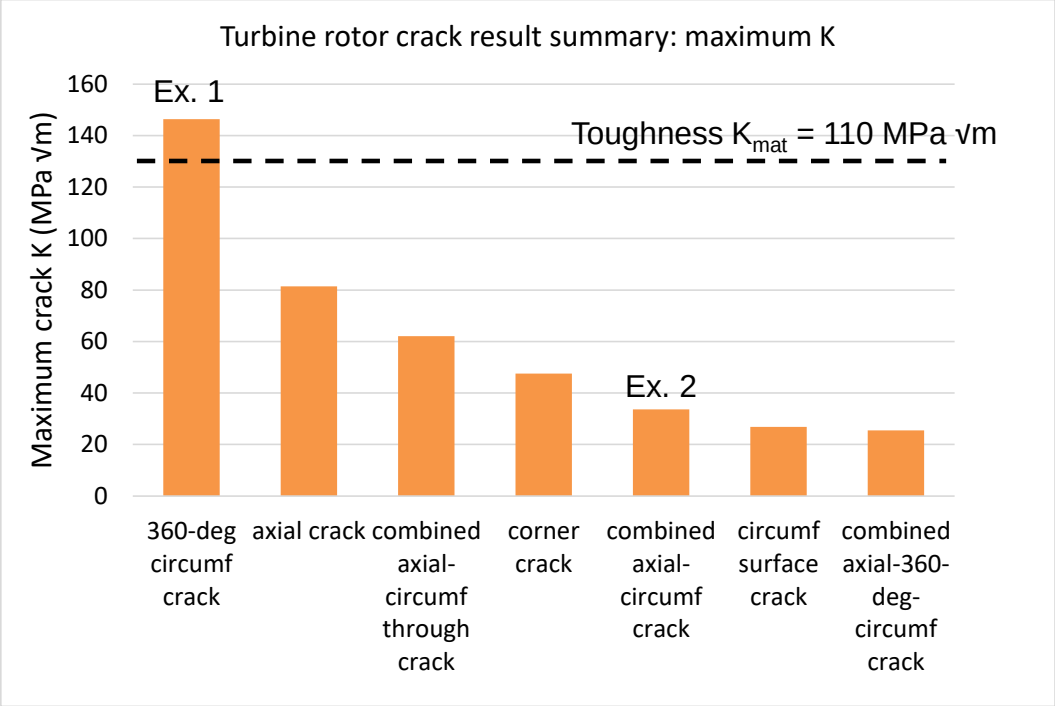

Figure 6. Crack ranking by maximum stress intensity.

2. Example 1: 360-degree Circumferential Crack

The first crack model example is shown in Figure 7, and shows the 1/8th symmetric shaft model with the 360-degree circumferential partial depth crack located in the steeple. The shaft rotates around the center axis, which is along the bottom edge of the mesh picture. Five circumferential crack depths were modeled: a = 4, 6, 8, 10, 12 mm.

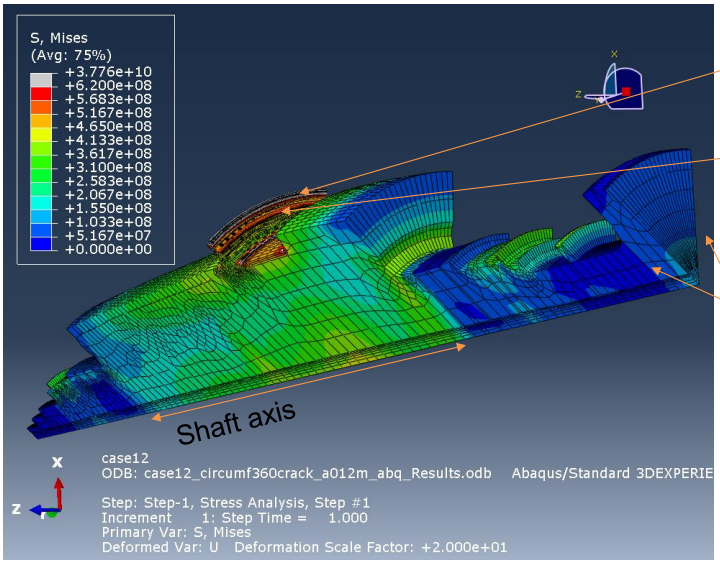

Figure 7. Example 1, 360-degree circumferential crack near the steeple top.

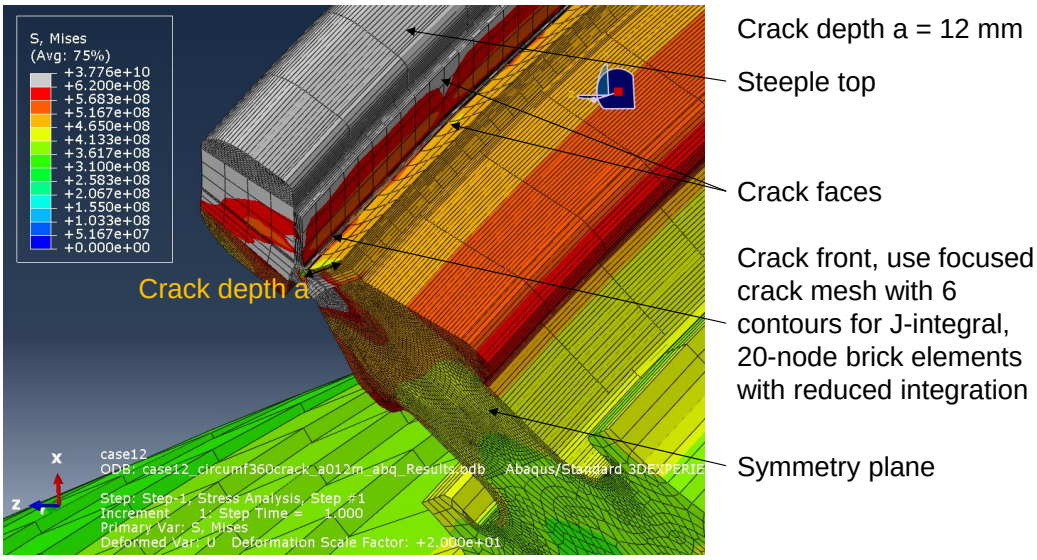

Figure 8. Ex. 1, 360-degree circumferential crack close-up, 20x displacement scale.

Figure 8 shows a close-up of the 360-degree circumferential crack near the top of the steeple for the crack depth a = 12 mm case. The crack depth, a, is measured from the near side of the steeple, across the steeple width, to the crack front. The centrifugal loads, pressures, and blade root block traction loads on the steeple ledges cause the crack to open. The 20x displacement scale shows the crack opening deformation. The crack front uses a focused mesh pattern, with collapsed brick elements at the crack front. Six concentric contours of brick elements are used to compute J-integral and stress intensity K values along the crack front using Abaqus/Standard. 20-node brick elements with reduced integration (Abaqus C3D20R element) are used in the crack mesh. The crack mesh is inserted into the larger turbine shaft model and connected using tied contact.

Figure 9 shows the stress intensity, K, trend versus the crack depth. The 12 mm deep crack case stress intensity exceeds the material's toughness, which was also seen in the bar chart in Figure 6. The deeper cracks will be examined further in Section 4 using the FAD method.

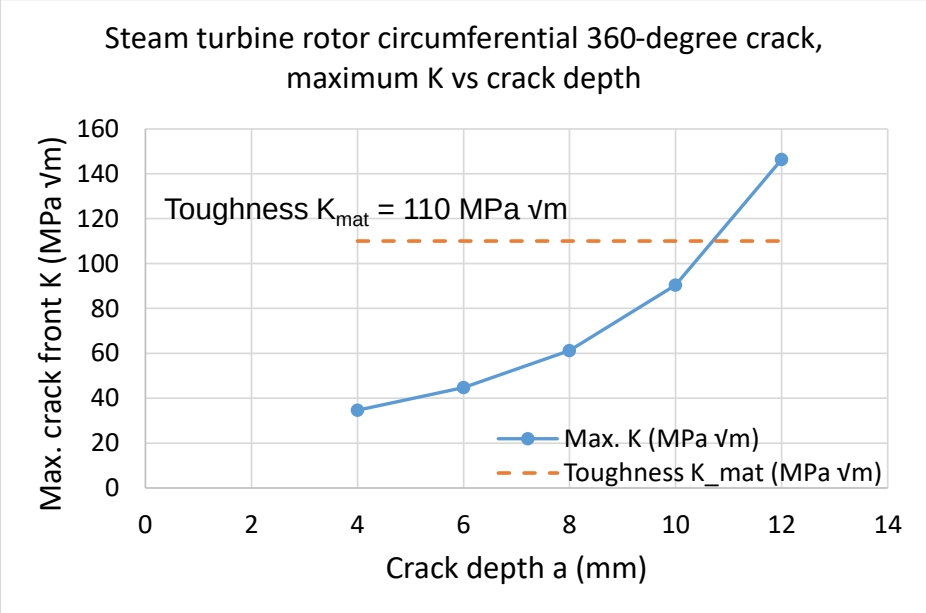

Figure 9. 360-degree circumferential crack stress intensity results.

3. Example 2: Combined Axial-Circumferential Crack

The second crack model example is shown in Figure 10, and is the combined axial-circumferential through crack. The axial crack segment extends from the top of the steeple to connect with the circumferential crack segment in the narrow part of the steeple. The top part of the steeple is

unconstrained to allow the axial crack segment to deform due to the applied loads. The axial crack segment length is kept constant at H = 14 mm from the top of the steeple to locate the circumferential through crack segment in the narrow region near the top of the steeple. The circumferential segment crack lengths are: c = 5, 10, 15 mm. The symmetry plane below the circumferential crack segment gives a model with a "T-shape" crack, where one side of the circumferential crack segment is modeled in the mesh. The crack mesh again uses a focused brick element mesh with six contours to compute the J-integral and stress intensity values along the crack front.

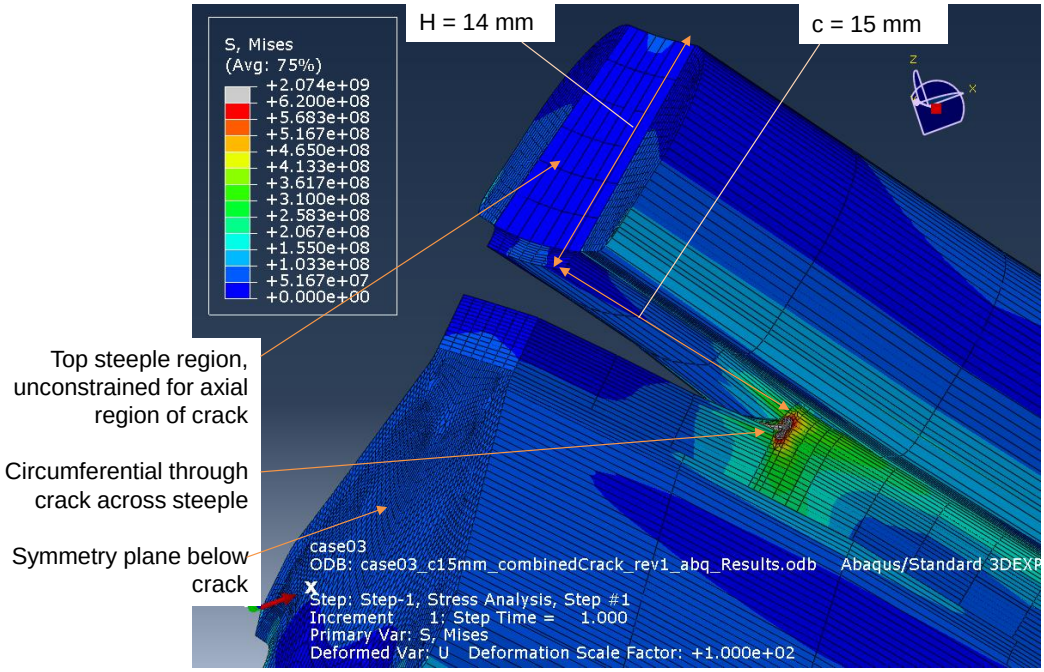

Figure 10. Example 2, combined axial-circumferential through crack model.

Figure 11 shows the crack front stress intensity results for three combined axial-circumferential through crack length cases. The K values are higher at the ends of the crack front at the free surfaces on each side of the steeple. The maximum K values are plotted versus the circumferential segment crack length in Figure 12, which shows the trend for this crack model has K values lower than the material toughness (horizontal dashed orange line). This combined crack shape example has lower K values than the first example, and is considered less severe than the 360-degree circumferential crack case.

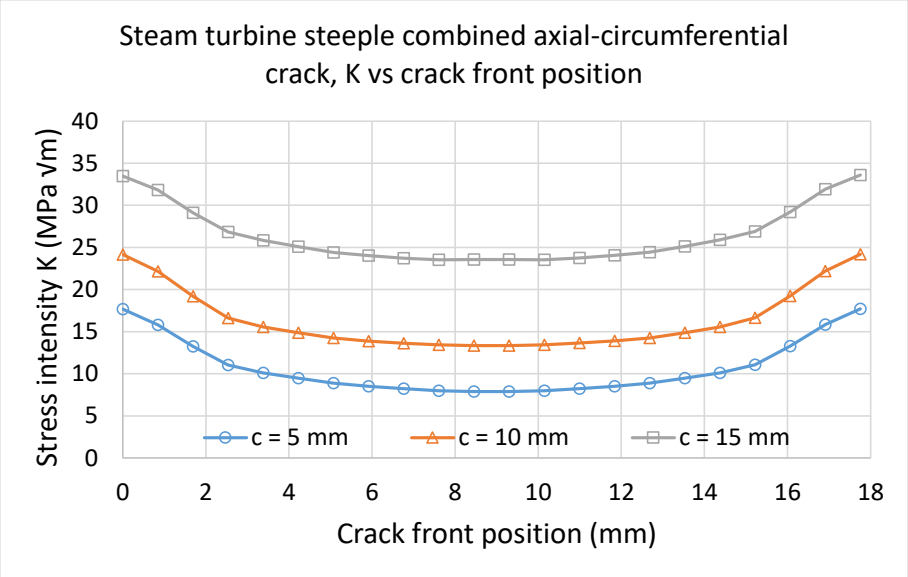

Figure 11. Combined axial-circumferential crack front stress intensity results.

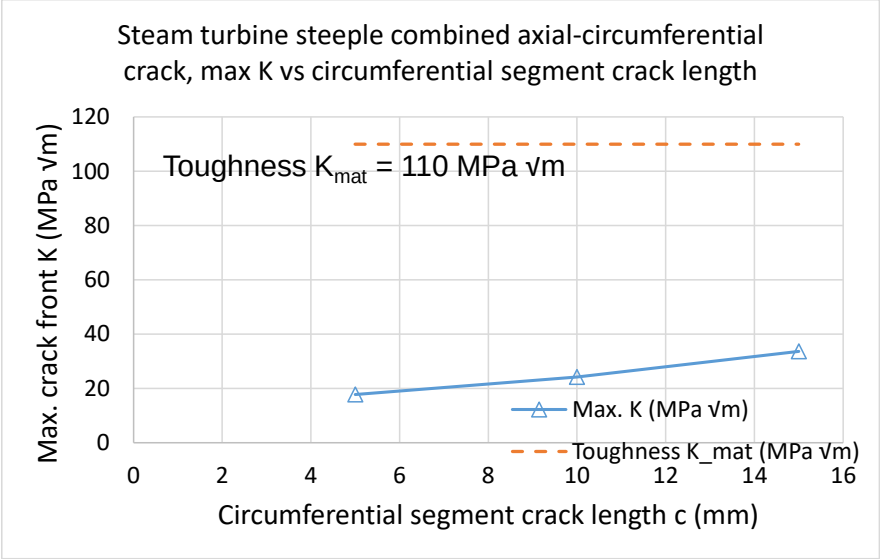

Figure 12. Combined axial-circumferential crack maximum K versus crack length.

4. Failure Assessment Diagram Method and Critical Crack Size

Of the crack cases examined in the turbine steeple, the 360-degree circumferential crack described in Example 1 gave the highest stress intensity values. The two deepest crack sizes are evaluated for failure using the Failure Assessment Diagram (FAD) method, which uses two non-dimensional ratios, Lr and Kr, to assess if a crack is stable or unstable (Anderson 2005, API 2016).

Figure 13 shows an example FAD. The x-axis Lr ratio evaluates plastic collapse and is computed from the reference stress divided by the yield strength. Computing the reference stress is described in more detail in the following paragraphs and figures. The FAD y-axis Kr ratio evaluates brittle fracture and is computed from the elastic stress intensity K divided by the material's toughness, K_{mat}.

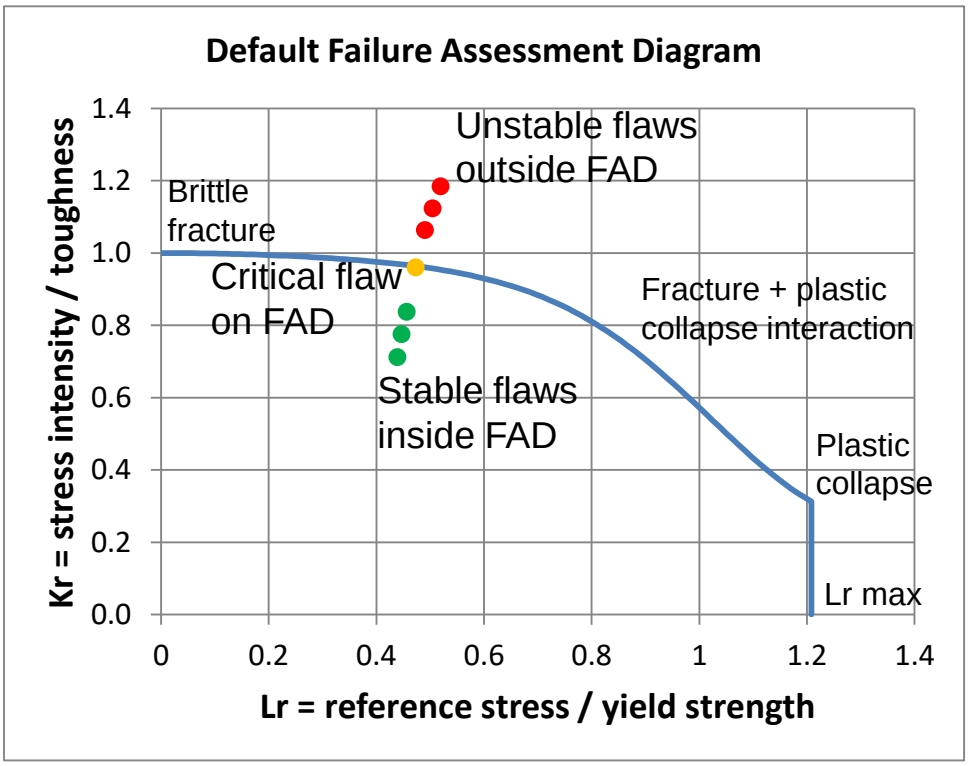

Figure 13. Example FAD plot for evaluating cracks for failure.

The FAD curve's shape accounts for the interaction between brittle fracture and plastic collapse. Lr,Kr assessment points inside the FAD curve are predicted to be stable (green points in Figure 13). Points on the FAD curve are critical (yellow point) and are on the verge of failure, which can

be useful to determine predicted critical crack sizes. Points outside the FAD curve, above the FAD or to the right of Lr_{max}, are predicted to be unstable (red points). It is possible for a crack to be unstable for Kr less than 1.0 if the Lr value is large enough to put the assessment point outside the FAD, so comparing just the crack front stress intensity to the material's toughness may not be sufficient to ensure that a crack is stable. The Lr_{max} cut-off value on the right side of the FAD limits the Lr value to check for plastic collapse, and it is typically given by the material flow stress (average of yield and tensile strengths) divided by the yield strength, although some materials have a specified Lr_{max}.

To determine FAD assessment points for the 360-degree circumferential cracks, an elastic-plastic Abaqus finite element analysis is used to compute the crack front J-integral for an increasing load amplitude. The non-linear material behavior is given by a stress-strain curve. The turbine rotor operating loads are multiplied by a common amplitude table to increase the loads enough to cause crack front plasticity. The focused mesh at the crack front is modified to use a set of initially coincident but unconnected crack front nodes to allow the crack front to blunt as the load increases. Figure 14 shows the plot of the crack depth a = 12 mm total J-integral results versus the load step index. The turbine's operating load is also the assessment load and is shown as load step 7. The elastic-plastic J-integral results are used to compute additional FAD values.

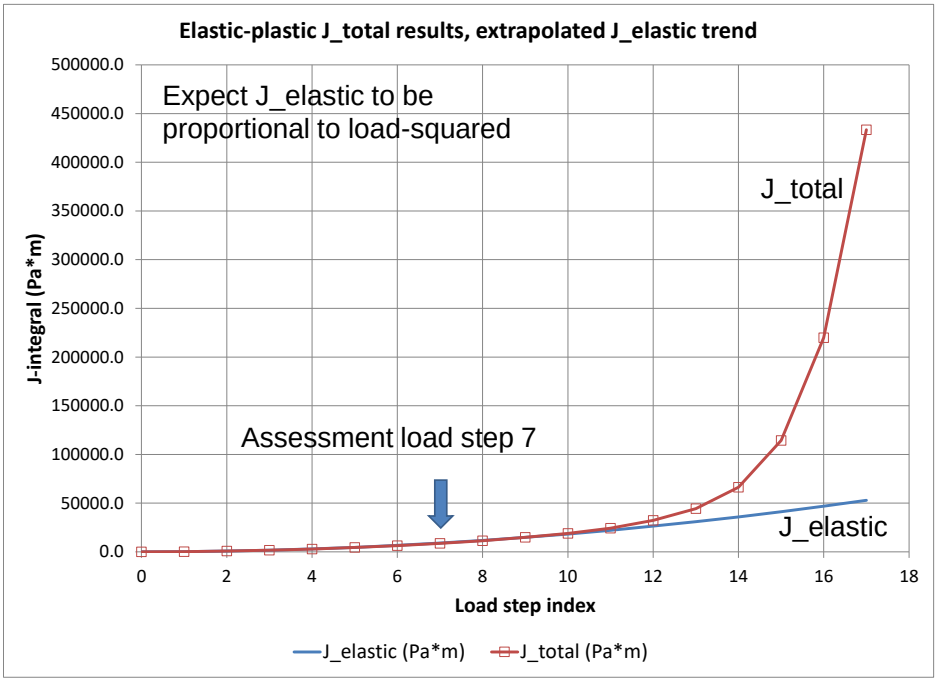

Figure 14. Total J-integral and elastic J results, 360-degree circumferential crack.

Another value needed to compute the FAD assessment points is the elastic part of the total J-integral. The elastic J-integral trend can be inferred from the first several load steps of the total J-integral, since the elastic J-integral is expected to be proportional to the load squared for the first several load steps. The load amplitude uses uniform increments so that the turbine shaft behavior is initially elastic. The first three load step J-integral values are used to compute a quadratic curve-fit for the elastic J-integral trend, and the next two load step J-integral values are used to confirm they are still following the elastic trend. Figure 14 shows that crack front plasticity is evident after step 10 where the total J-integral and elastic J-integral trends begin to diverge.

The total J-integral to elastic J-integral ratio trend is used to compute the nominal load, reference stress, and FAD curve by comparison to a material specific value given by Equation 1 (API 2016):

$$\left.\frac{J_{Total}}{J_{Elastic}}\right|_{Lr=1} = 1 + \frac{0.002E}{\sigma_{YS}} + 0.5\Big/\left(1 + \frac{0.002E}{\sigma_{YS}}\right) \tag{1}$$

where E is the modulus of elasticity and σ_{YS} is the 0.002 offset yield strength. For the steeple, the material specific value is 1.96.

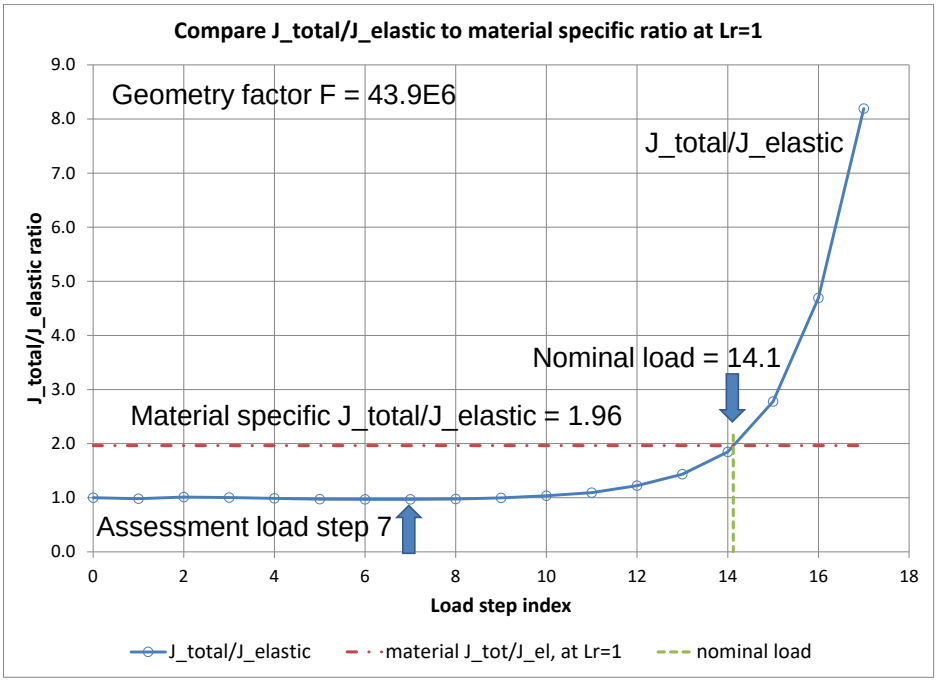

Figure 15. Determine nominal load using $J_{total}/J_{elastic}$ ratio.

Figure 15 shows the material specific value (horizontal dashed line) and trend for the ratio of the total J-integral to elastic J-integral. The intersection of these two curves gives the nominal load value of 14.1 (vertical dashed line) along the load step index x-axis.

The total J to elastic J trend is equal to 1 for the first 9 load steps while the turbine shaft behaves elastically in the analysis, then the ratio increases as crack front plasticity develops due to the increasing load magnitude. Enough crack front plasticity is needed to get the intersection with the material specific value so that the nominal load can be determined.

The reference stress geometry factor, *F*, is defined in Equation 2 as the ratio of the yield strength divided by the nominal load, $\sigma_{Nominal}$, and in this example the load step index is used as a generic nominal load value.

$$F = \frac{\sigma_{YS}}{\sigma_{Nominal}} \tag{2}$$

In this example, the geometry factor is 43.9E6. The reference stress σ_{ref} is computed using the geometry factor and load step index for every load increment σ_i in Equation 3:

$$\sigma_{ref} = F\sigma_i \tag{3}$$

The reference stress is used to compute the FAD curve Lr values at every load increment and to compute the Lr value at the evaluation load in Equation 4:

$$Lr = \frac{\sigma_{ref}}{\sigma_{YS}} = \frac{F\sigma_i}{\sigma_{YS}} \tag{4}$$

The FAD curve Kr values are computed at every load increment using the square-root of the ratio of the elastic J-integral divided by the total J-integral in Equation 5:

$$Kr = \sqrt{\frac{J_{Elastic}}{J_{Total}}} \tag{5}$$

The assessment point Kr value is computed from the elastic stress intensity K at the assessment load divided by the material's toughness K_{mat} in Equation 6:

$$Kr = \frac{K}{K_{mat}} \tag{6}$$

Figure 16 shows the FAD assessment points for the two deepest 360-degree circumferential cracks in the steeple, and their corresponding FAD curves. The 10 mm deep crack assessment point (blue circle) is below its FAD curve (blue dashed line) and is considered a stable sub-critical crack. The deeper 12 mm deep crack assessment point (red triangle) is above its FAD curve (red line) and is predicted to be an unstable crack that would cause failure. The computed FAD curves have the same general shape and trend, and may vary a small amount for each crack size. The FAD assessment points for the smaller cracks would be located below the 10 mm point, so they were omitted. T-stress could be used in a two-parameter fracture method to help identify the critical crack front location where instability would start a failure, but this is not yet an intrinsic part of the FAD method (ASTM).

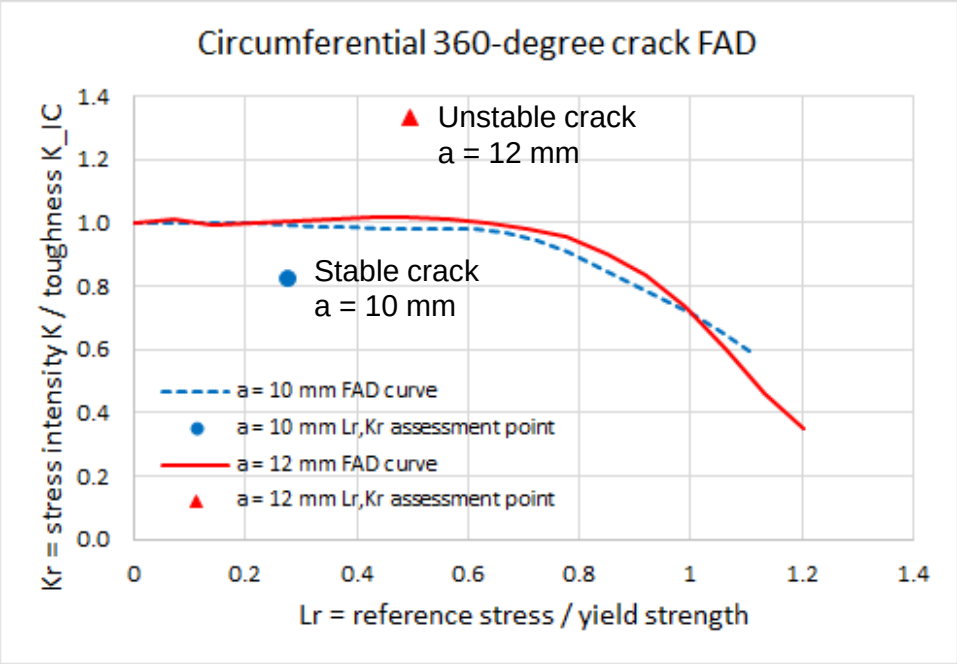

Figure 16. Evaluate two 360-degree circumferential crack depths on the FAD.

The FAD curves computed using the elastic-plastic J-integral results extend to the right side of the plot as far as the last converged analysis step. If needed to check plastic collapse, the FAD curves can be extended further to the right of the plot by rerunning the analysis to try and get J-integral results at higher loads, if the analysis will converge. An FAD assessment point typically shifts upward and to the right as the crack size increases. The Lr_{max} value could be applied to the FAD curves if the assessment point Lr values were further to the right side of the FAD.

More 360-degree circumferential crack models could be used to vary the crack depth between 10 and 12 mm to determine the predicted critical crack depth. However, these results were sufficient

to provide a stable crack depth of 10 mm that can help guide the turbine inspection planning to look for cracks in the steeple. If inspectors find cracking, the crack severity can be evaluated using additional 3D crack models and the FAD method.

5. Summary

This paper began by describing the steam turbine rotor shaft geometry and loading. The impulse wheel steeple is located near the middle of the shaft, and the seven postulated crack cases are located within the steeple. The postulated crack cases were ranked by the maximum crack front stress intensity K, where were computed using Abaqus/Standard finite element analyses. The 360-degree circumferential crack near the top of the steeple was the most severe crack case found.

Two crack analysis examples were examined in more detail, including the 360-degree circumferential crack model and the combined axial-circumferential crack model. The Failure Assessment Diagram (FAD) method was described and then used to evaluate the two deepest circumferential cracks for failure. The 10 mm deep circumferential crack is stable, and the 12 mm deep crack is unstable and predicted to cause a failure.

Using the crack ranking and FAD method identified the most severe crack case and will help inspectors look for cracks in the steeple during the maintenance shut-down. Being able to quantify crack severity using 3D crack models and the FAD method allow the turbine to return to operation with confidence in its structural integrity.

6. References

1. Abaqus User's Manual, Abaqus 3DEXPERIENCE R2017x, Dassault Systémes SIMULIA Corp., 1301 Atwood Ave., Suite 101W, Johnston, RI 02919.
2. Anderson, T. L., "Fracture Mechanics: Fundamentals and Applications", 3rd ed., 2005, CRC Press, Taylor & Francis Group, section 9.4.
3. API 579-1/ASME FFS-1, section 9G.4 "FAD-Based Method for Non-Growing Cracks", June 2016 "Fitness-For-Service", The American Society of Mechanical Engineers and the American Petroleum Institute, API Publishing Services, 1220 L Street, N.W., Washington, D.C. 20005.
4. ASTM E2899-13, "Standard Test Method for Measurement of Initiation Toughness in Surface Cracks Under Tension and Bending," Eq. A5.2, p. 22, ASTM International, 100 Barr Harbor Drive, PO Box C700, West Conshohocken, PA 19428.
5. FEACrack, version 3.2.32, 2017, Quest Integrity USA LLC, 1965 57th Court North, Suite 100, Boulder, Colorado, 80301, www.questintegrity.com.
6. Thorwald, G. and J. Wright, "Ductile Tearing Instability Assessment of a Cracked Reactor Pressure Vessel Nozzle for Larger Critical Crack Size Compared to the FAD Method," 2016 SIMULIA Science in the Age of Experience conference, May 2016, Boston, MA
7. Thorwald, G. and L. Parietti, "Leak-Before-Break Assessment of a Cracked Reactor Vessel Using 3D Crack meshes," Proceedings of the ASME 2016 Pressure Vessels and Piping Conference, PVP2016, July 17-21, 2016, paper no. PVP2016-63910.